Published in final edited form as:
Antivir Chem Chemother. ; 21(1): 1–14. doi:10.3851/IMP1680.

Nano-NRTIs: Efficient Inhibitors of HIV Type-1 in Macrophages with a Reduced Mitochondrial Toxicity

Serguei V. Vinogradov[1], **Larisa Y. Poluektova**[2], **Edward Makarov**[2], **Trevor Gerson**[1], and **Madapathage T. Senanayake**[1]

[1] Department of Pharmaceutical Sciences and Center for Drug Delivery and Nanomedicine, University of Nebraska Medical Center, Omaha, NE 68198, United States

[2] Center of Neurovirology and Neurodegenerative Disorders, University of Nebraska Medical Center, Omaha, NE 68198, United States

Abstract

Background—Macrophages serve as depot for HIV-1 in the central nervous system (CNS). To efficiently target macrophages, we developed nanocarriers for potential brain delivery of activated nucleoside reverse transcriptase inhibitors (Nano-NRTI).

Methods—Nanogel carriers consisting of PEG- or Pluronic-PEI biodegradable networks, star PEG-PEI, or PAMAM-PEI-PEG dendritic networks, as well as nanogels decorated with multiple ApoE peptide molecules, specifically binding to the apolipoprotein E receptor, were synthesized and evaluated. Nano-NRTIs were obtained by mixing aqueous solutions of triphosphates (AZTTP or ddITP) and nanocarriers followed by freeze-drying. Intracellular accumulation, cytotoxicity, and antiviral activity of Nano-NRTIs were monitored in monocyte-derived macrophages (MDMs). HIV-1_{ADA} viral activity in infected MDMs was measured by micro-RT assay following the treatment with Nano-NRTIs. Mitochondrial DNA (mtDNA) depletion in MDMs and human HepG2 cells was assessed by quantitative PCR (qPCR).

Results—Nanogels were efficiently captured by MDMs and demonstrated low cytotoxicity, not affecting viral activity without drugs. All Nano-NRTIs demonstrated high efficacy of HIV-1 inhibition at drug levels as low as 1 μmol/L, representing from 4.9 to 14-fold decrease in effective drug concentrations (EC_{90}) as compared to NRTIs, while cytotoxicity effects (IC_{50}) started at 200 times higher concentrations. Nanocarriers with core-shell structure and decorated with vector peptides (e.g. brain-targeting ApoE peptide) displayed the highest antiviral efficacy. The mtDNA depletion, a major cause of NRTI neurotoxicity, was reduced 3-fold compared to NRTIs at application of selected Nano-NRTIs.

Conclusions—Nano-NRTIs demonstrated a promising antiviral efficacy in MDMs and showed strong potential as nanocarriers for delivery of antiviral drugs to brain-harboring macrophages.

Keywords

nanogels; AZTTP; ddITP; HIV-1 infectivity; monocyte-derived macrophages; mitochondrial toxicity

Correspondence to: Serguei V. Vinogradov.

Introduction

Latent reservoirs of HIV-1 infection represent a significant obstacle in clearing the virus from infected patients and may result in the emergence of drug-resistant HIV-1 strains and a productive infection later in the disease progression. Macrophages are widely recognized as latently infected viral reservoirs and can be considered as critical HIV-1 target cells *in vivo* [1]. Significant work has been performed to establish antiviral activity of clinically approved NRTIs in macrophages; however, availability of many NRTIs to the treatment of macrophages in the central nervous system (CNS) was restricted by mechanisms of drug efflux in the blood-brain barrier (BBB) [2]. Additionally, treatment with therapeutic doses of NRTIs was found to be responsible for a secondary chronic neurotoxicity, the loss of neurons, with many observed effects that are incompletely understood, but already represent a rapidly growing problem with the current highly-active antiretroviral therapy (HAART) [3].

Targeted drug delivery and nanotechnology recently emerged as alternative approaches to reach HIV-1 in its natural reservoirs [4]. Although direct drug modification with brain-targeting moieties was discovered to be efficient for overcoming the BBB in a number of applications, it may result in a significant reduction of drug activity [5]. Fortunately, nanoparticles could safely deliver significant drug payloads and were efficiently captured by various types of macrophages following systemic administration [6]. Targeted nanoparticles also held a high promise for drug delivery across the BBB to the brain [7]. Various types of nanocarriers were proposed for delivery of antiretroviral drugs, including nucleoside analogs (NRTIs), although mostly in a non-phosphorylated form [8]. However, since 5′-triphosphates of nucleoside analogs (NATP) are the active drug species and chain terminators of DNA or RNA synthesis, delivery of these compounds into HIV-1 infected cells may add significantly to the efficacy of antiviral chemotherapy compared to current NRTIs [9]. Initial attempts at the liposomal delivery of 5′-triphosphates of antiviral nucleoside analogs were published in the 1990s [10–11]. Red blood cells were also proposed as NATP drug delivery vehicles [12]. Lately, soft cationic nanogels [13–14] and polymeric nanocapsules [15–16] have been successfully evaluated as other types of nanocarriers for 5′-triphosphates of cytotoxic and antiviral drugs. Nanogels demonstrated efficient cellular accumulation and cytosolic drug release, and their surface could be decorated with various vector molecules, including brain-targeting moieties [17]. In the current study, we demonstrated for the first time an efficient application of hydrophilic nanocarriers, cationic nanogels, loaded with activated antiviral drugs, 5′-triphosphates of NRTIs (Nano-NRTIs) for inhibition of HIV-1 replication in macrophages. In addition to the observed higher antiviral efficacy, Nano-NRTIs proved to be the drug nanoformulations with a reduced mitochondrial toxicity as compared to free drugs. We hypothesize that Nano-NRTIs can be efficient for an *in vivo* transport of NRTIs across the BBB via targeting of brain-specific apolipoprotein E receptor in order to reach latent HIV-1 reservoirs in the CNS.

Methods

1. Chemistry

Materials—Most of reagents and solvents, including the hydroxypropyl PAMAM dendrimer G(5) were purchased from Sigma-Aldrich (St. Louis, MO) and used without additional purification. [5-^{3}H]-Thymidine 5′-triphosphate (20–25Ci/mmol) was purchased from Moravek Radiochemicals (Brea, CA). Pluronic F-68 was obtained as generous gift from BASF (Partispany, NJ). The bifunctional linker MAL- PEG_{5000}-NHS was purchased from GenKem Technology USA (Allen, TX). 75-armed star PEG 423 was obtained from Shearwater, Inc. (Huntsville, AL). ATP BODIPY FL was purchased from Molecular Probes-Invitrogen (Carlsbad, CA). Zidovudine (AZT) and didanosine (ddI) were obtained from AK

Scientific (Mountain View, CA). Mouse apolipoprotein E-derived peptide, CGLRKMRKRLMR with C-amide protection, was custom synthesized by Biomer Technologies (Pleasanton, CA), purified by semi-preparative reverse-phase HPLC and used for nanogel decoration (12).

Synthesis of nanogels—Cationic nanogel networks PEG-*cl*-(ss)PEI (NG1) and Pluronic F68-*cl*-(ss)PEI (NG2) were synthesized starting from biodegradable disulfide-bridged polyethylenimine (ss)PEI using previously described methods [13,18]. Star PEG (75 arms, Mw 450,000) was activated by 1,1′-carbonyldiimidazole and then modified with an excess of branched PEI (Mw 2,000) to obtain a cationic starPEG-*g*-PEI network (NG3). Carboxylated PAMAM dendrimer G(5) was activated by water-soluble carbodiimide (EDC) and then modified with an excess of PEG-*g*-PEI conjugate (mPEG, Mw 5,000/branched PEI, Mw 1,200) to obtain a cationic PAMAM-PEI-*g*-PEG network (NG4). Swollen NG1-NG4 networks are schematically shown in Figure 1A. All nanocarriers were fractionated by size exclusion chromatography on a column with Sephacryl S-300 (1.5 × 60 cm), using an elution buffer containing 0.2M sodium chloride, 20mM sodium acetate, pH 6, and 20% ethanol, and a refractive index flow detector. Fractions containing nanogel dispersions with a diameter < 220nm were collected, desalted by dialysis against water, filtered through 0.22μm sterile filter, and freeze-dried.

ApoE peptide-modified nanogel was prepared as follows. Nanogel NG1 (25 mg) was dissolved in 0.5 mL water, then solution of a MAL-PEG_{5000}-NHS linker (10 mg/0.5 mL) was added, and the mixture was incubated for 2 h at 25°C. Without isolation, a 2-fold excess (5 mg) of ApoE peptide was added in 0.5 mL DMF and the pH was reduced to 6 by 3M sodium acetate, pH5.5. The reaction was continued overnight at 4°C. Peptide-modified nanogel was isolated by size-exclusion chromatography using a Sephacryl S-300 column equilibrated in 0.2M sodium chloride, 20mM sodium acetate, pH6, in 20% ethanol. The product, ApoE-NG1, was desalted by dialysis (Mw cutoff 8–12kDa) and lyophilized. Peptide content was determined using an automatic aminoacid analyzer (Applied Biosystems, Foster City, CA).

Synthesis of triphosphates—Nucleoside analogs zidovudine (AZT) and didanosine (ddI) were phosphorylated and triphosphorylated using a previously reported one-batch method [19]. 5′-Triphosphate products, AZTTP and ddITP, were purified by anion-exchange chromatography on DEAE-Sephadex A-25 with a gradient of ammonium acetate in 20% ethanol, desalted by dialysis (Biotech SpectraPor, Mw cutoff 500 Da) and lyophilized. The HPLC and UV-purity of these compounds was analyzed by analytical ion-pair HPLC, alkaline phosphatase hydrolysis, and UV absorbance at 260 nm [19]. Spectral characteristics (proton and phosphorus NMR) and analytical HPLC profiles of these products can be found in the Supplemental Material Section (on-line).

Preparation of Nano-NRTIs—Briefly, equal volumes of aqueous solutions of nanogel (80mg/mL) and triphosphate (20mg/mL) were mixed together and incubated for 60 min in ice bath. The forming Nano-NRTIs were separated from non-complexed nucleosides by gel-filtration on a NAP-10 column equilibrated in deionized water and freeze-dried. The calculated drug content (μg nucleoside per 1 mg of Nano-NRTI formulation) was based on the measured UV absorbance at 260nm and extinction coefficients (ε_{260}) of the corresponding nucleosides: AZT 9,700, ddI 8,100, and cytidine 9,000 (Table 1). Nano-NRTIs were stored as dry formulations refrigerated and used after dissolving in sterile water before treatment.

2. Virology

Primary human monocyte isolation and HIV-1 infection—Monocytes were obtained from leukopheresis of HIV-1, HIV-2 and hepatitis B seronegative donors and purified by countercurrent centrifugal elutriation as previously described [20]. Cells were cultured in DMEM supplemented with 10% heat-inactivated pooled human serum and 1% glutamine (Sigma-Aldrich, St. Louis, MO), 10 mg/mL ciprofloxacin (Sigma-Aldrich), and 1000 U/ml of purified recombinant human macrophage colony stimulating factor (MCSF). A macrophage-tropic viral strain HIV-1_{ADA}, at a multiplicity of infection (MOI) of 0.01, was amplified as previously described [21]. This laboratory-adapted strain was selected following a prior extensive analysis of macrophage function and neurotoxicity based on strain differences. The levels of viral growth of the HIV-1_{ADA} strain were nearly uniform and not dependent on host cell differences. This ensured that the data acquired would be reproducible from one experiment to another regardless of the macrophage donor.

Cellular uptake—Nanogels were tagged with rhodamine isothiocyanate and purified using a NAP-10 column (GE Healthcare Life Sciences, Piscataway, NJ) as described previously [17]. Fluorescent nanogels NG1-NG4 were loaded with a model 5′-triphosphate (CTP, 20% wt) to neutralize positive charges, isolated on a NAP-10 column and lyophilized. Nanogel solutions (4 mg/mL) were dispensed in full cellular medium to a 96-well plate to obtain the concentration 20 μg/mL. At appropriate time intervals, equal volumes of the MDM suspension (1×10^6 cells/mL) in full medium were added. The treated cells were washed with cold PBS and centrifuged twice, resuspended with propidium iodide (10 μl) and incubate for 15 minutes at 4°C before the flow cytometry analysis. The percentage of live cells and mean fluorescent intensity was measured using FACS Array Bioanalyzer (BD Bioscience, Franklin Lakes, NJ).

For confocal microscopy studies, a Rho-NG1 was loaded with a fluorescent triphosphate, ATP *BODIPY FL*, as described above for CTP. MDMs were treated separately with a Rho-NG1/ATP *BODIPY FL* formulation, a Rho-NG1 alone (10 μg/mL), and ATP BODIPY FL (1 μg/mL) in full cellular medium for 1 h at 37°C. MDMs were washed several times with cold PBS, centrifuged and fixed with paraformaldehyde. Confocal microscopy was performed in covered chamber slides using a Zeiss 410 Confocal Laser Scanning Microscope equipped with an argon-krypton laser (UNMC Confocal LSM Core Facility).

Antiviral effects evaluation—Human MDMs were cultured for 7 days in 96-well plates, changing culture medium every other day. Nano-NRTIs and NRTIs were dissolved in sterile deionized water to obtain 20x stock solutions. In sterile 96-well plate, 10 μl of 20x stock solutions were mixed with 190 μl of complete macrophage culture medium, and serial 1/2 dilutions (100 μl) were prepared at AZT and ddI concentrations from 16 to 0.5μg/ml. On Day 7, 100 μl of old media was removed and supplemented with the serial dilutions of NRTIs or Nano-NRTIs in full medium (100 μl). Plates were incubated for 2 or 4 h at 37oC and 5% CO_2. After incubation supernatants were carefully aspirated, cells were washed with 200 μl of PBS, and the fresh media containing 0.01 MOI of HIV-1_{ADA} was added for the overnight (16 h) infection. MDMs were then washed, supplemented with a fresh medium and incubated for additional 7 days. On Day 5 and 7 post-infection, supernatants were collected for RT assay. Each plate contained infected (non-treated with drug) and uninfected (treated with culture medium alone) cell controls. All drugs concentrations and controls were analyzed in 5 parallels.

To measure HIV-1 replication, reverse transcriptase (RT) activity was determined by incubating 10 μL of infected sample media with a reaction mixture consisting of 0.05% Nonidet P-40 (Sigma-Aldrich) and [^{3}H]-dTTP (2 Ci/mmol; Moravek, Brea, CA) in Tris-HCl

buffer (pH 7.9) for 24 h at 37°C on days 5 and 7 post-infection [21]. Radiolabeled DNA was precipitated on paper filters in an automatic cell harvester (Skatron, Sterling, VA) and incorporated activity was measured by liquid scintillation spectroscopy. The cytotoxicity of NRTIs and Nano-NRTIs to MDMs was determined on Day 7 using an MTT assay as previously described [22]. The mean OD_{490} values for non-treated controls were taken for 1, and other cytotoxicity data have been converted correspondingly to obtain the normalization factors. All observed HIV RT activity values were divided by these normalization factors, and the adjusted HIV RT activity (cpm/mL) was plotted as a function of drug concentrations. Antiviral efficacy of NRTI and Nano-NRTI was expressed as the effective drug concentration that inhibited HIV-1 RT activity by 90% (EC_{90}) and was determined from concentration-effect curves generated using GraphPad Prism 4.03 (GraphPad Software, San Diego, CA).

Mitochondrial DNA analysis—Effect of NRTIs and Nano-NRTIs on the content of mitochondrial DNA was measured following the prolonged treatment of MDMs using a SYBR Green real-time PCR method. Cells were treated with sterile solutions of AZT, AZT +ddI, AZTTP or AZTTP+ddITP-loaded nanogels at two drug concentrations (15 and 30 μg/mL) in full medium for 4h at 37°C on Days 1, 4, 7 and 10, and analyzed on Day 14. HepG2 cells (ATCC, Manassas, VA) were cultured as previously described [18]. The medium was renewed after every treatment. After trypsinolysis and treatment with RNase, DNA samples were isolated using the FujiFilm Quickgene DNA Tissue Kit S and Mini80 extraction cartridges. The obtained DNA samples were quantified and had A_{260}/A_{280} ratios in a recommended range.

Human cytochrom *b* gene primers (mtDNA): 5′-CCAACATCTCCGCATGATGAAAC-3′ (direct) and 5′-GTGGGCGATTGATGAAAAGG-3′ (reverse), and β-actin gene primers (nuDNA): 5′-AACACCCCAGCCATGTACGT-3′ (direct) and 5′-TCTCCTTAATGTCACGCACGA-3′ (reverse) were used in the PCR analysis [23]. All primers were synthesized and cartridge-purified in the UNMC Eppley Molecular Biology Core Facility. SYBR Green Real-Time PCR reactions were performed in quadruplicates using the MiniOpticon Real-Time PCR detection system (BioRad, Hercules, CA). The PCR reaction mixtures contained an equal amount of DNA (10–20ng in 5μL) determined by UV-absorbance, 5μL of 2μM primer mix and 10μL of BioRad SsoFast Evagreen Supermix. PCR conditions were as follows: an initial denaturation at 98°C for 2 min, followed by amplifications at 98°C at 95°C for 15s, and 60°C for 1 min (40 cycles) and a melting/annealing cycle. The quality of primers and conditions of amplification were checked at different dilutions of isolated DNA, and the efficacy of amplification was close to 0.9. The results were calculated as the content of mtDNA normalized to the content of nuclear DNA: $m = 2^{-C(t)mt}/2^{-C(t)nu}$, where $C(t)_{mt}$ and $C(t)_{nu}$ are the quantification cycles observed for mtDNA and nuDNA in each sample. MtDNA content in non-treated cells was taken for 100%, and all obtained data were expressed as the percentage change of the mtDNA content compared to non-treated cells.

Statistical analysis—All experiments were performed at least two-three times in duplicates. Data are presented as mean ± SEM. The experimental data were analyzed using unpaired Student's t-test. Results were considered significant at $P < 0.05$, with a two-tailed test.

Results

Preparation of Nano-NRTIs

Nanogel networks with an even spatial distribution of cationic and neutral polymeric molecules (NG1), a layered structure and cationic polymer in outer layer (NG2 and NG3), and a cationic core-neutral shell structure (NG4) were prepared in order to compare their efficacy in the delivery of 5′-triphosphates of antiviral nucleoside analogs to macrophages (Figure 1A). All these networks had a high ratio of neutral to cationic polymers to ensure lower cytotoxicity of nanocarriers, and the total nitrogen content measured by elemental analysis was 2.2 μmol/mg nanogels on average (Table 1). Biodegradable segmented PEI with disulfide bridges was used in the synthesis of nanogels NG1 and NG2 [18]. Following the reduction of disulfide bridges inside the cells, these nanogels are capable to quick degradation to nontoxic PEG/Pluronic-*g*-PEI conjugates (Mw < 30 kDa), which can be effectively removed by kidneys. For modification with a brain-specific peptide vector, ApoE-receptor binding peptide [24], nanogels were initially treated with a bifunctional PEG linker and then with an N-cystein-ApoE peptide C-amide. Efficiency of the coupling reaction was usually not less than 70%. The maleimide-thiol linkage between PEG and peptide is stable *in vivo*, as well as the C-protected linear peptide attached to PEG molecule. The peptide-modified nanogels were previously shown to efficiently bind brain capillary endothelial cells in culture and accumulate in the brain *in vivo* (data are to be published elsewhere).

All nanogels were well-swollen in water, forming stable transparent dispersions after ultrasonication. Nucleoside 5′-triphosphate (NTP) molecules easily penetrated into nanogel pores and spontaneously bound to the cationic PEI chains in the network after simple mixing of both aqueous solutions, forming compact particles with a dense drug-loaded core and PEG molecules in the protective outer layer (Figure 2). The hydrodynamic diameter of all nanogels in water was less than 200 nm. The dispersed nanogel networks demonstrated a very low light scattering efficacy in aqueous dispersions before being associated with anionic drugs, when they formed compacted drug-loaded core-shell particles with 1.5-2-fold smaller diameter of 100 nm in average. Usually, a condensed core of 30–50nm in diameter formed, therefore a protective PEG layer could be a twice as thick [13]. The NTP-loaded nanogels were separated from an unbound triphosphate by gel filtration; drug loading capacity was calculated based on UV absorbance and molar extinction coefficients of each nucleoside and expressed in μg of nucleoside per 1 mg of the formulation (Table 1). Theoretical NTP binding in nanogels calculated on the basis of their total nitrogen analysis was very close to the observed average drug content value (13% or 0.28μmol/mg).

Cellular accumulation

Rhodamine (Rho) isothiocyanate-labeled nanogels were used to study their capture by macrophages. Initially, Rho-NG1 was loaded with a fluorescent 5′-triphosphate, ATP *BODIPY FL*, using the same protocol as for NRTIs, and the obtained double-labeled nanoformulation (100 μg/mL) was used to treat MDMs for 2 h at 37°C. No cytotoxicity was evident during the treatment of MDMs (IC_{50} of the nanogel NG1: 0.3 mg/mL). Fast and efficient capture of free and ATP *BODIPY FL*-loaded fluorescent nanogel particles was observed by confocal microscopy, showing their prevalent cytoplasmic accumulation. Conversely to Rho-labeled nanogel, accumulation level of free ATP *BODIPY FL* in macrophages was noticeably lower (Figure 3A:a,b). Superposition pictures of both labels also demonstrated an intensive process of intracellular release of the triphosphate from nanogels in the cytoplasm, which is visible as a diffuse green fluorescence (Figure 3A:c,d). Co-localized triphosphate and nanogel are visible in yellow dotted areas, evidently encompassed in endosomes. These results directly confirm that nanogel-delivered

triphosphates can be available in free form for virus inhibition in macrophages very quickly after the beginning of the treatment.

The capture of all types of nanogels by MDMs has been investigated by flow cytometry. There we observed a significant difference in the cell accumulation rate among the various Rho-labeled nanogels (10μg/mL). The fastest capture was observed for nanogel NG3, which was followed by NG1, while NG2 and NG4 showed equally lower capture efficacy (Figure 3B). These differences can be explained by various PEG densities and charge shielding in these nanogels. The first pair (NG1 and NG3) seems to have formed networks with a positive charge on their surface and less uniform and dense outer PEG layer, while the second pair (NG2 and NG4) formed more condense particles with the cationic core and expanded outer PEG layer. The first type of nanogel architecture should simplify binding with serum proteins (opsonisation) and the consequent recognition by macrophages, but the second type of architecture has more protection against protein coating and the corresponding capture by macrophages. It is worth to note, that although the macrophage capture of NG3 is nearly 2-fold higher and NG1 − 50% higher, as compared to NG2 and NG4, the overall antiviral activity may depend not only on the nanogel capture, but on efficacies of both nanogel uptake and drug release processes, as showed in the following experiments with HIV-1 infected MDMs.

Antiviral efficacy

Nano-NRTIs were examined for their ability to inhibit HIV-1 replication in an *in vitro* model system using infected MDMs. The cells were pre-treated for 2–4 h with either free drug (AZT or ddI) or Nano- NRTIs containing AZTTP, ddITP or AZTTP+ddITP at concentration from 0.25 to 30 μg/mL, washed and inoculated with HIV-1_{ADA} at MOI 0.01. Culture supernatants were monitored for viral replication by measuring reverse transcriptase (RT) activity by inclusion of ^{3}H-TTP on days 5 and 7 post-infection using a micro-RT assay. The RT data were normalized for cytotoxicity of free and Nano-NRTIs determined using an MTT assay. In preliminary experiments, we found that preincubation time had a visible affect on antiviral efficacy of Nano-NRTIs; the strongest antiviral effect was obtained at a longer incubation time (Figure 4A). It is evident from Figure 3 that cellular uptake of nanogels did not reach plateau after 2 h of incubation; a longer time should increase the internalization of nanogels and also the release of activated drug molecules from nanogels into the cytoplasm. Because of different cytotoxicities of nanogels, we compared antiviral effect of Nano-NRTIs mostly at 2h-preincubation time in order to reduce any effects associated with cytotoxicity of nanocarriers. The nanogels by themselves displayed no visible antiviral activity (Figure 4B). Most of the studied Nano-NRTIs were relatively non-cytotoxic to MDMs that showed no signs of cytotoxicity up to Nano-NRTI concentrations of 100–200 μg/mL. Both Nano-AZTTPs and Nano-ddITPs demonstrated more efficient suppression of HIV RT activity than corresponding NRTIs (AZT and ddI) at equivalent drug concentrations (0.25, 0.5, 1 and 2 μg/mL) by comparison of the IC_{90} values calculated from these dose-effect curves adjusted for cytotoxicity (Figures 4C). The IC_{90} data presented in Table 2 have been calculated from three separate experiments where these “drug-effect” curves were obtained.

All investigated Nano-NRTIs showed strong anti-HIV effect at the effective drug concentration (EC_{90}) as low as 0.5 μg/mL (Table 2). All EC_{90} values were calculated from the data obtained from three or four independent experiments with HIV-1 infected MDMs. Corresponding free drugs showed similar activity at concentrations from 3.9 (AZT) to 7 μg/mL (ddI). For Nano-AZTTPs, the enhancement was 2.6–4.9-fold, while for Nano-ddITP, it reached a 3.4–14-fold values. Nearly complete eradication of virus by selected Nano-NRTIs, when <1% viral activity was detected, could be reached at drug concentrations of only 2–4 μg/mL, even though treatment with free drugs at these concentrations was strikingly

ineffective (Figure 4C). Modification of nanogels with the brain-specific ApoE peptide (AP) had a little effect on the observed antiviral efficacy, and both AP-NG1/AZTTP and AP-NG1/ddITP at lowest studied drug concentrations (0.25 μg/mL or 1 μmol/L) demonstrated a nearly 2-fold higher antiviral efficacy (Figure 4D). Commonly, levels of antiviral activity of Nano-AZTTPs were close for NG1, NG2 and NG3 (1.5–1.6 μg/mL), having the best EC_{90} values for NG4 (1 μg/mL) and AP-NG1 (0.8 μg/mL or 3 μmol/L) (Table 2). Nano-ddITPs demonstrated the best results for NG2 (0.6 μg/mL) and NG4 (0.5 μg/mL or 2 μmol/L), while NG1, AP-NG1 and NG3 showed EC_{90} values between 1.6 and 2.1 μg/mL. The two-drug combination, AZT+ddI (1:1 w/w), was slightly more efficient (3.6 μg/mL) than AZT or ddI alone (3.9 and 7 μg/mL, respectively), as well as the NG1/AZTTP+ddITP nanoformulation (0.9 vs. 1.5 and 1.6 μg/mL). However, for the vectorized AP-NG1/AZTTP+ddITP, EC_{90} value was merely an average of EC_{90} values for AP-NG1/AZTTP and AP-NG1/ddITP (1.2 vs. 0.8 and 1.7 μg/mL, respectively) (Table 2). Summarizing all above, it is evident that mostly Nano-NRTIs with a core-shell structure, such as nanogel NG4, or peptide-decorated AP-NG1, displayed the highest antiviral efficacy (EC_{90} below 1 μg/mL, or 4 μmol/L).

Mitochondrial toxicity

Mitochondrial toxicity of NRTIs results from the depletion of mitochondrial DNA (mtDNA), which occurs because of the mtDNA chain growth termination or inhibition of DNA polymerase gamma [25]. In order to compare NRTIs and Nano-NRTIs and evaluate their influence on mitochondrial toxicity, we measured the relative amount of mtDNA in macrophages after two weeks-long treatment using real-time PCR. Additionally, mitochondrial toxicity was analyzed at similar conditions in human hepatocyte HepG2 cells, a widely-accepted cellular model for drug toxicity studies [23]. Cells have been treated with drugs and drug-loaded nanogels (15 or 30 μg/mL of AZT or AZT+ddI, 1:1, w/w) for 4 h at 37°C every three days over a two-week period (four doses). The total DNA was isolated from treated samples, and then a SYBR Green qPCR analysis of mtDNA and nuDNA was performed in quadruplicates. In MDMs, the effect of AZT treatment was nearly zero at concentration 15μg/mL, while the corresponding AZT+ddI combination resulted in 50% reduction of the mtDNA level (Figures 5A and 5B). Unexpectedly, the NG3/AZTTP nanoformulation revealed significant mtDNA depletion in MDMs (75%). Additionally, when a control NG3 nanoformulation without drug was tested, we obtained the same level of mtDNA depletion. Evidently, it means that the structure of nanogel NG3 has a specific adverse effect on the mitochondria function in MDMs. All other Nano-NRTIs demonstrated no mtDNA depletion in the result of the treatment; on the contrary, they posted a 25–100% increase in the mtDNA content over non-treated MDMs. One plausible explanation could be a macrophage activation accompanied by a rise in the number of mitochondria. Previously, we also observed an unexplained increase in the formazan level during a MTT cytotoxicity assay of MDMs treated with selected Nano-AZTTPs or Nano-ddITPs (Figure 5D). Then, the strongest increase was detected for NG1/AZTTP and NG2/AZTTP. Similarly, we obtained the highest activation of MDMs and increase in the mtDNA content after the treatment by NG1/AZTTP (+105%) and NG2/AZTTP (+60%) nanoformulations (Figure 5A). AP-NG1/AZTTP and NG4/AZTTP demonstrated a moderate MDMs activation (30–40%). All observed data were statistically significant ($P < 0.05$, over AZT).

Then, we tested an effect of Nano-NRTIs containing a 1:1 mixture of AZTTP and ddITP on the mtDNA content in MDMs treated with drug doses of 15–30 μg/mL (Figure 5B). ApoE peptide-modified AP-NG1/AZTTP+ddITP showed a low mitochondrial toxicity after 14 days of treatment, affecting the mtDNA content in dose-dependent manner by +60% (15 μg/mL) and by −14% (30 μg/mL) over non- treated MDMs. In general, the effect of AP-NG1/AZTTP+ddITP was similar to the effect of AP-NG1/AZTTP on MDM activation (+50 and +30%, respectively).

Conversely, we did not observe any increase in the mtDNA content after the treatment of HepG2 cells with free AZT and Nano-AZTTPs at drug concentrations 15 μg/mL (Figure 5C). The two-weeks treatment by AZT resulted in significant mtDNA depletion (80%), while selected Nano-AZTTPs reduced mtDNA depletion to only 25–33%; NG1, AP-NG1 and NG3 being the most effective nanocarriers. The mtDNA content was nearly identical after the treatment with NG1 (75%, $P < 0.01$), AP-NG1/AZTTP (52%, $P < 0.05$), and NG3/AZTTP (64%, $P < 0.001$), while differences between them have been not significant (*NS*). Both NG2/AZTTP and NG4/AZTTP demonstrated higher mitochondrial toxicities (57–62% depletion, $P < 0.05$). Evidently, the mtDNA depletion may at least in part be a nanocarrier-specific. The observed protective effect of selected Nano-AZTTPs versus AZT on mitochondria can be explained by a low efficacy of triphosphate transport from cytoplasm through the mitochondrial membrane. The general conclusion from these results is that an efficient shielding of positive charge in Nano-NRTIs may play a decisive role in the mitochondrial toxicity of nanocarriers and activation of MDMs. Thus, peptide-modified AP-NG1 and the core-shell NG4 showed the best characteristics in general, while unmodified nanogels NG1, NG2 and NG3, having a high density of positively charged molecules in outer layer, demonstrated the highest mitochondrial toxicity and MDM activation.

Discussion

Highly active antiretroviral therapy (HAART) has greatly improved survival and quality of life of the AIDS patients, but did not reduce the recurrence of the disease because of HIV-1 hiding in the brain. Treatment of latent HIV-1 harbored in the brain, mostly in macrophages, has proven to be a challenge using the HAART. Many of current antiviral drugs cannot penetrate the BBB because of the activity of various drug efflux transporter proteins in the brain capillary endothelial cells (BCEC) forming the barrier. Development of novel less toxic drugs and effective drug nanoformulations, which are able to deliver antiviral drugs to the latent HIV-1 reservoirs, is now considered as the first priority in anti-HIV drug research [26]. Moreover, chronic exposure of peripheral neurons to NRTIs during the treatment often results in the gradual neurotoxic degradation of patients [27]. Chronic neurotoxicity, liver damage, lipodistrophy, and myopathy are now recognized as major HAART associated complications. Mitochondrial toxicity of many antiviral NRTIs, which affect the activity of DNA polymerase gamma and the mitochondria function, and incorporate into mtDNA, resulting in the mtDNA depletion, is now considered a major cause of these complications [28–30].

Development of nanosized drug delivery systems has shown tremendous potential for enhancement of drugs penetration across the BBB [31,32]. Recent progress in the design of hydrophilic micro- and nanogels made them promising drug carriers together with liposomes, nanoparticles and micellar formulations [33]. Cationic nanogels demonstrated a strong ability to enhance drug penetration across the BBB and could be efficiently vectorized to the brain using through a receptor-mediated binding [17]. In this report, we evaluated anti-HIV efficacy of nanogel formulations of AZTTP and ddITP, active triphosphate species of antiviral NRTIs, zidovudine and didanosine, in the *in vitro* system of HIV-1 infected macrophages. Delivery of active NRTIs offers an advantage of the fast antiviral effect through bypassing the intracellular phosphorylation steps of drug activation. Lately, several groups have reported application of nanocarriers for delivery of antiviral nucleoside 5′-triphosphates. Hillaireau *et al* formulated the PEI-associated AZTTP into hollow polyisobutylcyanoacrylate nanocapsules and demonstrated a 30-fold increase in cellular uptake of the encapsulated drug [15]. Kohli *et al* showed a 30-fold enhancement of antiviral activity and 10-fold increase in selectivity index of nanogel-encapsulated ribavirin 5′-triphosphate compared to free ribavirin in influenza virus-infected MDCK cells [18]. Saiyed *et al* demonstrated an efficient AZTTP delivery in liposomes and suppression of

HIV-1 replication in peripheral blood mononuclear cells, as well as a CNS delivery of magnetic liposomes encapsulating AZTTP [34,35]. Here, we observed a fast capture of nanogels by MDMs; triphosphate drug-loaded nanogels exhibited a sufficient drug release in the cytosol already in 60 min after the capture, so that therapeutic levels of activated NRTIs could be reached in MDMs very fast and at subtoxic concentrations of Nano-NRTIs.

Nanogels represent the hydrophilic type of nanocarriers, which have evident advantages before liposomes for systemic administration and drug delivery to the BBB. The hydrophilic nature and high dispersion stability of drug-loaded nanogels, together with their ability of crossing the BBB, make nanogels a convenient platform for the development of vectorized brain-targeted drug nanoformulations. The second feature of cationic nanogels is the ability to encapsulate 5′-triphosphates of different nucleoside analogs and efficiently carry them inside various types of cells [14]. The active phosphorylated form of AZT, AZTTP, was shown to induce a lower mitochondrial toxicity than free AZT when delivered in HepG2 cells in the form of NG1/AZTTP formulation [18].

The ability of different Nano-NRTIs to reduce mitochondrial toxicity of NRTIs during a prolonged treatment was confirmed in cultured MDMs and human hepatocyte HepG2 cells. According to Azzam *et al* [36], treatment by AZT (up to 25 μg/mL, or 0.1 mM) did not affect the mtDNA content in MDMs, but could result in potent mitochondrial toxicity in other tissues/cells (e.g., muscles, heart, liver), while ddI had one of the highest potency of the inhibition of polymerase gamma in mitochondria among NRTIs. Although we observed no effect of AZT and a moderate effect of AZT+ddI mixture on the mtDNA content in MDMs, an substantial increase in mtDNA content was detected after the prolonged treatment by many of Nano-NRTIs (Fig. 5A and 5B). We hypothesize that the treatment with selected nanocarriers might provoke an activation of macrophages. Phagocytosis is energy-dependent process, and macrophages derive most of this energy from glucose metabolism and oxidative phosphorylation in mitochondria. Activation of MDMs can result in the increased mitochondrial numbers, the fact noted by some researchers [37]. Detrimental effect of higher doses of NRTIs can impair phagocytic activity of MDMs; however, it may be compensated by an increase in mitochondrial numbers. We also observed a significant 2-fold increase in the formation of formazan, the product of MTT conversion by mitochondrial enzymatic activities, during the cytotoxicity assay of HIV-infected MDMs treated with NG1/AZTTP and NG2/AZTTP (Fig.5D). Taken together, both results on mtDNA content and MTT conversion activity suggest a significant 2-fold increase in amount of mitochondria following the treatment of MDMs by the above-mentioned Nano-NRTIs. Another cellular model for drug cytotoxicity studies, human HepG2 cells, did not show this effect, and all Nano-AZTTPs demonstrated from 2 to 3.2-fold lower depletion in mtDNA compared to free AZT at the equivalent drug dose. The lower hepatotoxicity of Nano-NRTIs is additionally enhanced by nanogel *in vivo* biodistribution properties. Although the *i.v.*-injected nanogels were capable of liver accumulation in some extent, this accumulation was usually lower compared to many other nanocarriers, such as liposomes [17]. Generally, the surface PEGylation could reduce interaction of nanocarriers with plasma proteins and increase circulation times [33]. Here, we observed the highest antiviral activity of nanogels with a core-shell structure, and nanocarriers with peptide modification. These types of Nano-NRTIs are evidently worth of further development to obtain targeted nanocarriers for systemic applications. Core-shell architecture is one of the most promising ways to diminish the non-specific organ accumulation and toxicities of nano-NRTIs.

In order to develop an effective antiviral therapy against HIV-1 reservoirs in the brain, investigators face three major problems associated with systemically administered nanocarriers, such as a highly polarized *in vivo* biodistribution, inefficient brain targeting, and unspecific cellular and neurotoxicity. Only preliminary steps have been made in the area

of design and evaluation of brain-targeted drug nanoformulations. Most of currently available nanocarriers in the non-targeted form are effectively captured by peripheral macrophages of the lung, spleen and liver; therefore, their CNS delivery is far from optimal. Recently, several applications of apolipoprotein E (ApoE)-decorated nanoparticles or nanocarriers modified with ApoE receptor-binding peptides were described, which have demonstrated an increased brain accumulation compared to non-modified carriers [38–40]. Here, we suggested that a placement of multiple copies of short ApoE peptide molecules on the surface of nanogel could result in more specific binding of nanogels with the BBB receptors and lower nonspecific biodistribution. As a first step, here, we demonstrated that decoration of nanogels with ApoE peptides does not diminish the antiviral efficacy of Nano-NRTIs in HIV-infected macrophages. This result makes us optimistic about the ensuing *in vivo* applications of vectorized Nano-NRTIs. *In vivo* evaluation of selected brain-targeted Nano-NRTIs is currently under way in an established mouse model of NeuroAIDS.

Supplementary Material

Refer to Web version on PubMed Central for supplementary material.

Acknowledgments

This work was supported by NIH grants NS063879 and CA136921 to S.V.V. Authors are grateful to the very helpful output of UNMC Flow Cytometry, Confocal Microscopy, and Oligonucleotide Synthesis Core facilities.

References

1. Gavegnano C, Schinazi RF. Antiretroviral therapy in macrophages: implication for HIV eradication. Antiviral Chem Chemother 2009;20:63–78.
2. McGee B, Smith N, Aweeka F. HIV pharmacology: barriers to the eradication of HIV from the CNS. HIV Clin Trials 2006;7:142–53. [PubMed: 16880170]
3. Cherry CL, McArthur JC, Hoy JF, Wesselingh SL. Nucleoside analogues and neuropathy in the era of HAART. J Clin Virol 2003;26:195–207. [PubMed: 12600651]
4. Vyas TK, Shah L, Amiji MM. Nanoparticulate drug carriers for delivery of HIV/AIDS therapy to viral reservoir sites. Expert Opin Drug Deliv 2006;3:613–628. [PubMed: 16948557]
5. Temsamani J, Rousselle C, Rees AR, Scherrmann JM. Vector-mediated drug delivery to the brain. Expert Opin Biol Ther 2001;1:773–782. [PubMed: 11728213]
6. Chellat F, Merhi Y, Moreau A, Yahia L. Therapeutic potential of nanoparticulate systems for macrophage targeting. Biomaterials 2005;26:7260–75. [PubMed: 16023200]
7. Garcia-Garcia E, Andrieux K, Gil S, Couvreur P. Colloidal carriers and blood-brain barrier (BBB) translocation: a way to deliver drugs to the brain? Int J Pharm 2005;298:274–292. [PubMed: 15896933]
8. Hillaireau H, Le Doan T, Couvreur P. Polymer-based nanoparticles for the delivery of nucleoside analogues. J Nanosci Nanotechnol 2006;6:2608–17. [PubMed: 17048470]
9. Painter GR, Almond MR, Mao S, Liotta DC. Biochemical and mechanistic basis for the activity of nucleoside analogue inhibitors of HIV reverse transcriptase. Curr Top Med Chem 2004;4:1035–1044. [PubMed: 15193137]
10. Szebeni J, Wahl SM, Betageri GV, Wahl LM, Gartner S, Popovic M, Parker RJ, Black CD, Weinstein JN. Inhibition of HIV-1 in monocyte/macrophage cultures by 2′,3′-dideoxycytidine-5′-triphosphate, free and in liposomes. AIDS Res Hum Retroviruses 1990;6:691–702. [PubMed: 2163269]
11. Oussoren C, Magnani M, Fraternale A, Casabianca A, Chiarantini L, Ingebrigsten R, Underberg WJ, Storm G. Liposomes as carriers of the antiretroviral agent dideoxycytidine-5′-triphosphate. Int J Pharm 1999;180:261–270. [PubMed: 10370196]

12. Magnani M, Rossi L, Fraternale A, Casabianca A, Brandi G, Benatti U, De Flora A. Targeting antiviral nucleotide analogues to macrophages. J Leukoc Biol 1997;62:133–137. [PubMed: 9226004]
13. Vinogradov SV, Zeman AD, Batrakova EV, Kabanov AV. Polyplex Nanogel formulations for drug delivery of cytotoxic nucleoside analogs. J Control Release 2005;107:143–157. [PubMed: 16039001]
14. Vinogradov SV. Polymeric nanogel formulations of nucleoside analogs. Expert Opin Drug Deliv 2007;4:5–17. [PubMed: 17184158]
15. Hillaireau H, Le Doan T, Appel M, Couvreur P. Hybrid polymer nanocapsules enhance in vitro delivery of azidothymidine-triphosphate to macrophages. J Control Release 2006;116:346–52. [PubMed: 17113178]
16. Hillaireau H, Le Doan T, Chacun H, Janin J, Couvreur P. Encapsulation of mono- and oligo-nucleotides into aqueous-core nanocapsules in presence of various water-soluble polymers. Int J Pharm 2007;331:148–152. [PubMed: 17150318]
17. Vinogradov SV, Batrakova EV, Kabanov AV. Nanogels for oligonucleotide delivery to the brain. Bioconjug Chem 2004;15:50–60. [PubMed: 14733583]
18. Kohli E, Han HY, Zeman AD, Vinogradov SV. Formulations of biodegradable Nanogel carriers with 5′-triphosphates of nucleoside analogs that display a reduced cytotoxicity and enhanced drug activity. J Control Release 2007;121:19–27. [PubMed: 17509713]
19. Vinogradov SV, Kohli E, Zeman AD. Cross-linked polymeric nanogel formulations of 5′-triphosphates of nucleoside analogues: role of the cellular membrane in drug release. Mol Pharm 2005;2:449–461. [PubMed: 16323952]
20. Gendelman HE, Orenstein JM, Martin MA, et al. Efficient isolation and propagation of human immunodeficiency virus on recombinant colony-stimulating factor 1-treated monocytes. J Exp Med 1988;167:1428–1441. [PubMed: 3258626]
21. Nukuna A, Gendelman HE, Limoges J, et al. Levels of human immunodeficiency virus type 1 (HIV-1) replication in macrophages determines the severity of murine HIV-1 encephalitis. J Neurovirol 2004;10 (Suppl 1):82–90. [PubMed: 14982744]
22. Reardon JE, Miller WH. Human immunodeficiency virus reverse transcriptase. Substrate and inhibitor kinetics with thymidine 5′-triphosphate and 3′-azido-3′-deoxythymidine 5′-triphosphate. J Biol Chem 1990;265:20302–20307. [PubMed: 1700787]
23. Hoschele D, Wiertz M, Moreno IG. A duplex real-time PCR assay for detection of drug-induced mitochondrial DNA depletion in HepG2 cells. Anal Biochem 2008;379:70–72.
24. Sauer I, Dunay IR, Weisgraber K, Bienert M, Dathe M. An apolipoprotein E-derived peptide mediates uptake of sterically stabilized liposomes into brain capillary endothelial cells. Biochemistry 2005;44:2021–2029. [PubMed: 15697227]
25. Chiao SK, Romero DL, Johnson DE. Current HIV therapeutics: mechanistic and chemical determinants of toxicity. Curr Opin Drug Discov Devel 2009;12:53–60.
26. Rao KS, Ghorpade A, Labhasetwar V. Targeting anti-HIV drugs to the CNS. Expert Opin Drug Deliv 2009;6:771–784. [PubMed: 19566446]
27. Nowacek A, Kosloski LM, Gendelman HE. Neurodegenerative disorders and nanoformulated drug development. Nanomedicine (Lond) 2009;4:541–55. [PubMed: 19572820]
28. Inductivo-Yu I, Bonacini M. Highly active antiretroviral therapy-induced liver injury. Curr Drug Saf 2008;3:4–13. [PubMed: 18690975]
29. Mallewa JE, Wilkins E, Vilar J, Mallewa M, Doran D, Back D, Pirmohamed M. HIV-associated lipodystrophy: a review of underlying mechanisms and therapeutic options. J Antimicrob Chemother 2008;62:648–660. [PubMed: 18565973]
30. Scruggs ER, Dirks Naylor AJ. Mechanisms of zidovudine-induced mitochondrial toxicity and myopathy. Pharmacology 2008;82:83–8. [PubMed: 18504416]
31. Nowacek A, Gendelman HE. NanoART, neuroAIDS and CNS drug delivery. Nanomed 2009;4:557–574.
32. Wong HL, Chattopadhyay N, Wu XY, Bendayan R. Nanotechnology applications for improved delivery of antiretroviral drugs to the brain. Adv Drug Deliv Rev 2010;62:502–17.

33. Kabanov AV, Vinogradov SV. Nanogels as pharmaceutical carriers: finite networks of infinite capabilities. Angew Chem Intern Ed 2009;48:5418–29.
34. Saiyed ZM, Gandhi NH, Nair MP. Magnetic nanoformulation of azidothymidine 5′-triphosphate for targeted delivery across the blood-brain barrier. Int J Nanomed 2010;5:157–66.
35. Saiyed ZM, Gandhi NH, Nair MP. AZT 5′-triphosphate nanoformulation suppresses human immunodeficiency virus type 1 replication in peripheral blood mononuclear cells. J Neurovirol 2009:1–5. (epubl). [PubMed: 19462266]
36. Azzam R, Lal L, Goh S-L, Kedzierska CL, Jaworowski A, Naim E, Cherry CL, Wesselingh SL, Mills J, Crowe SM. Adverse effects of retroviral drugs on HIV-1-infected and uninfected human monocyte-derived macrophages. Acquir Immune Defic Syndr 2006;42:19–28.
37. Daigneault M, Preston JA, Marriott HM, Whyte MK, Dockrell DH. The identification of markers of macrophage differentiation in PMA-stimulated THP-1 cells and monocyte-derived macrophages. PLoS One 2010;5:e8668. [PubMed: 20084270]
38. Göppert TM, Müller RH. Polysorbate-stabilized solid lipid nanoparticles as colloidal carriers for intravenous targeting of drugs to the brain: comparison of plasma protein adsorption patterns. J Drug Target 2005;13:179–187. [PubMed: 16036306]
39. Leupold E, Nikolenko H, Dathe M. Apolipoprotein E peptide-modified colloidal carriers: the design determines the mechanism of uptake in vascular endothelial cells. Biochim Biophys Acta 2009;1788:442–449. [PubMed: 19121285]
40. Zensi A, Begley D, Pontikis C, Legros C, Mihoreanu L, Wagner S, Büchel C, von Briesen H, Kreuter J. Albumin nanoparticles targeted with ApoE enter the CNS by transcytosis and are delivered to neurones. J Control Release 2009;137:78–86. [PubMed: 19285109]

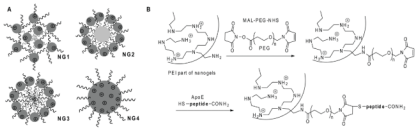

Figure 1.

(**A**) Structural types of nanogel carriers used in the study: PEG-*cl*-PEI(ss) (**NG1**), F68-*cl*-PEI(ss)(**NG2**), star PEG-*g*-PEI (**NG3**) and PAMAM-PEI-*g*-PEG(**NG4**). (**B**) Synthesis of the ApoE peptide-decorated nanogel NG1 by the attachment of bifunctional PEG linker to amino groups in the PEI backbone, following with a maleimide moiety modification by N-cysteine-ApoE peptide C-amide.

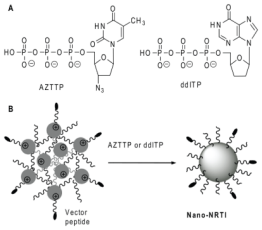

Figure 2.
(**A**) Chemical structures of antiviral nucleoside 5′-triphosphates AZTTP and ddITP. (**B**) Formation of Nano-NRTIs by self-association of negatively charged triphosphates with cationic nanogel network in aqueous solution.

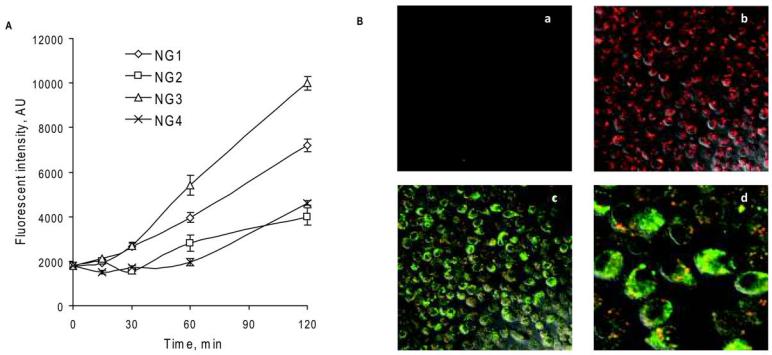

Figure 3.

Cellular accumulation of nanogels in MDMs. (**A**) Kinetics of the accumulation of Rh-labeled nanogels by flow cytometry data (means ± SEM, n = 2). (**B**) Confocal pictures of MDMs treated for 2 h at 37°C with a fluorescent ATP-BODIPY FL (**a**), rhodamine-labeled nanogel Rho-NG1(**b**), and nanoformulation Rho-NG1/ATP-BODIPY FL (**c**, **d**).

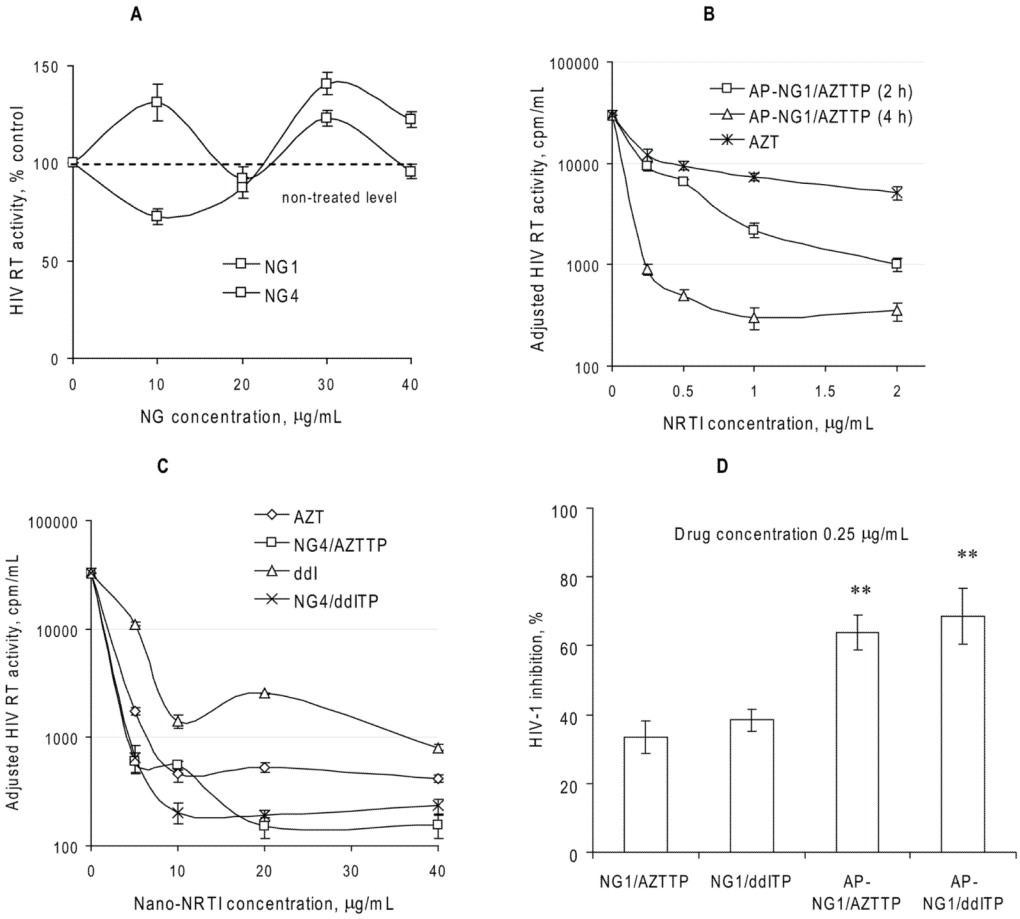

Figure 4.

Antiviral activity of Nano-NRTIs in HIV-1 infected MDMs. (**A**) HIV RT activity measured in cultural media on Day 5 after infection of MDMs pre-incubated for 2 h with nanogels without drug at concentrations 10–40 μg/mL (means ± SEM, n = 5). Activity in non-treated infected cells was taken for 100%. (**B**) Dose-dependent antiviral effect of AP-NG1/AZTTP pre-incubated with MDMs for 2 or 4 h at 37°C (means ± SEM, n = 5). HIV RT activity was adjusted by normalization using cytotoxicity data (MTT assay). (**C**) Antiviral effect-dose curves for Nano-NRTIs (for example, NG4/AZTTP and NG4/ddITP) and corresponding NRTIs (AZT and ddI) pre-incubated with MDMs for 2 h at 37°C (means ± SEM, n = 5). These curves were used for calculation of EC_{90} values presented in Table 2. (**D**) HIV-1 inhibition by non-vectorized and vectorized Nano-NRTIs. HIV RT activity was compared in MDMs after the pre-incubation for 4 h at 37°C with AZTTP and ddITP-loaded nanogels containing equal amount of drugs (0.25 μg/mL of AZT or ddI) followed by HIV-1 infection. Data are shown as means ± SEM (n = 5); (**) $P < 0.01$ between the corresponding non-vectorized and AP-vectorized Nano-NRTIs.

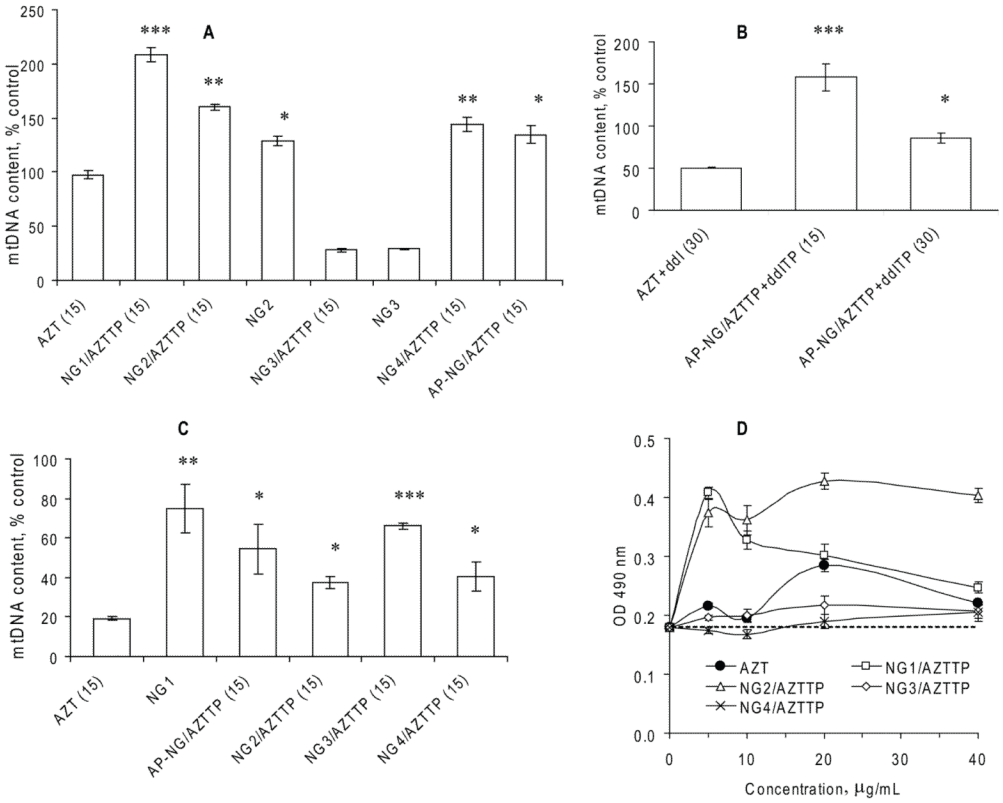

Figure 5.

Mitochondrial toxicity of Nano-NRTIs in MDMs and HepG2 cells. (**A**) Mitochondrial (mt) DNA content in MDMs treated with three doses of corresponding Nano-AZTTPs (at AZT concentration of 15 μg/mL) or nanogels without drugs for 14 days at 37°C. qPCR data for mtDNA were normalized by a reference gene data and presented as percentage of the mtDNA level in non-treated MDMs taken for 100% (means ± SEM, n = 5); (*) $P < 0.001$, (**) $P < 0.01$, and (*) $P < 0.05$ between AZT group and Nano-NRTIs or nanogels. (**B**) mtDNA content in MDMs treated with AZT+ddI (1:1 w/w) mixture and corresponding AP-NG/AZTTP+ddITP formulations at two doses 15 and 30 μg/mL, as described above (means ± SEM, n = 5); (*) $P < 0.001$, and (*) $P < 0.05$ between AZT+ddI group and Nano-NRTIs. (**C**) mtDNA content in HepG2 cells treated as described above (means ± SEM, n = 5); (*) $P < 0.001$, (**) $P < 0.01$, and (*) $P < 0.05$ between AZT group and Nano-NRTIs or nanogels. (**D**) Absorbance of the formazan product (OD 490 nm) observed in a MTT cytotoxicity assay of HIV-infected MDMs treated with AZT or Nano-AZTTPs (means ± SEM, n = 5). Absorbance level for non-treated HIV-infected cells is shown by the dotted line.

Table 1

Properties of nanogels and Nano-NRTI

	Network	Total N content, mmol/mg*	Hydrodynamic diameter, nm†	NTP content in Nano-NRTIs,%‡		
				AZTTP	ddITP	CTP
NG1	PEG-*cl*-PEI*ss*	2.5	175 ± 10 (90 ± 3)	23	8.5	13.5
NG2	F68-*cl*-PEI*ss*	2.1	190 ± 7 (120 ± 9)	16	6.5	11
NG3	starPEG-*g*-PEI	1.8	150 ± 9 (115 ± 5)	21	11.5	15.5
NG4	PAMAM-PEI-*g*-PEG	2.2	160 ± 7 (100 ± 6)	12	5.5	13
AP-NG1	ApoE-NG1	1.9	197 ± 11 (105 ± 5)	16	8	9.5

*Determined by elemental analysis of nanogels

†Measured by DLS (water, pH 7, concentration 0.1%). Data for NTP-loaded nanogels are shown in brackets

‡Determined by UV absorbance of aqueous solutions of NTP-loaded nanogels and free drugs at 260 nm

Table 2

Antiviral effect (EC_{90}) of the treatment of HIV-infected MDMs with Nano-NRTIs

	EC_{90} (AZT, μg/mL)*		**EC_{90} (ddI, μg/mL)***		**EC_{90} (AZT+ddI, μg/mL)***
AZT	3.9 ± 0.3	ddI	7.0 ± 0.4	AZT + ddI	3.6 ± 0.5
NG1/AZTTP	1.5 ± 0.4	NG1/ddITP	1.6 ± 0.3	NG1/AZTTP+ddITP	0.9 ± 0.3
AP-NG1/AZTTP	0.8 ± 0.5	AP-NG1/ddITP	1.7 ± 0.4	AP-NG1/AZTTP+ddITP	1.2 ± 0.2
NG2/AZTTP	1.5 ± 0.3	NG2/ddITP	0.6 ± 0.2		
NG3/AZTTP	1.6 ± 0.3	NG3/ddITP	2.1 ± 0.5		
NG4/AZTTP	1 ± 0.2	NG4/ddITP	0.5 ± 0.1		

*EC_{90} values (means ± SEM) were calculated from the dose-effect curves obtained for each drug/nanoformulation in three-four independent experiments